Two-electron cusp in the double ionization of helium

L. Gulyás and L. Sarkadi
Institute of Nuclear Research of the Hungarian Academy of Sciences (ATOMKI), H-4001 Debrecen, Post Office Box 51, Hungary

A. Igarashi
Department of Applied Physics, Faculty of Engineering, University of Miyazaki, 889-2192, Japan

T. Kirchner
Department of Physics and Astronomy, York University, 4700 Keele Street, Toronto, Ontario, Canada M3J 1P3
(Received 11 June 2010; published 10 September 2010)

We analyze the double ionization of He under the impact of 100 keV He^{2+} projectiles. The process is described within the framework of the impact parameter and frozen-correlation approximations where the one-electron events are treated by the continuum distorted wave method. Correlation between the emitted electrons, which plays an important role in forming the shape of the differential distribution of the electron emission, is described by the Coulomb density of states approximation (CDS). Special attention is paid to the region of the two-electron cusp that has been observed in a recent experiment for 100 keV He^0 + He collisions [L. Sarkadi and A. Orbán, Phys. Rev. Lett. **100**, 133201 (2008)]. In the cusp region the correlated motion of the two electrons is influenced dominantly by the outgoing projectile, that is, the correlation function of the CDS treatment is expected to depend on the electron momenta measured relative to the projectile rather than to the target nucleus. A qualitative agreement with the experiment is achieved with a CDS model based on the use of such a projectile-centered correlation function that applies effective charges as given in the dynamically screened three-Coulomb wave function.

DOI: 10.1103/PhysRevA.82.032705 PACS number(s): 34.70.+e

I. INTRODUCTION

The double ionization (DI) of He has been investigated intensively in recent years [1–3]. The interest arises from the opportunity of studying the correlated motion of two electrons in the field of a heavy Coulomb particle. This situation emerges most cleanly in the reaction of photo-double-ionization where at nonrelativistic photon energies the momentum transferred by the photon is negligible, and the ejection of the second electron is due to the electron-electron interaction [2]. Two electrons in the continuum can also be investigated in the electron-impact DI of the He atom, commonly known as the $(e,3e)$ process [1]. Most of the $(e,3e)$ studies were performed at high impact energies where a fast (identified as the scattered projectile) and two slow electrons specify the most interesting part of the final channel [4]. For both the photon and electron impacts, first-order theories (dipole and first Born approximations) provide adequate tools for the description of the ejection mechanism [5], while the three-body character cannot be neglected for the proper account of the final two-electron continuum. One popular approximation for the treatment of the final double continuum is given by the *three-Coulomb* (3C) wave function [6,7]. This wave function is derived by the diagonalization of the three-body Hamiltonian and has the correct asymptotic behavior when all interparticle distances are large. The 3C wave function has the advantage of being analytical so that it is practical to apply it in studies of DI in various systems. Numerous applications have shown that the models based on the 3C wave function can reproduce most of the observed features of the cross sections, however, its validity breaks down for some particular kinematical configurations. One such configuration appears above the threshold region, known as the domain of the Wannier theories, where the two slow electrons emerge in the opposite direction [8]. The theoretical account of the process requires a very accurate description of the so-called Wannier ridge in the full three-body potential where the two electrons are supposed to be staying as roughly equidistant from the nucleus [2,9]. At the same time, the framework of the 3C approximation enables a relatively simple, although not unique, tool to extend the validity of the 3C ansatz to the threshold region. This is based on the realization that the three-body screening effects are not represented in the 3C wave function [10]. One of the simplest ways is the replacement of the fixed charges of the particles by dynamically screened effective charges depending upon the relative coordinates or momenta of the outgoing particles, known as the *dynamically screened* 3C (DS3C) approximation [11].

The process of DI of He by ion impact also received considerable interest in recent years [12,13]. A variety of projectiles, fully stripped and dressed ions from low to relativistic energies together with antiprotons, are available for these studies. Although remarkable progress has been made in exploring the different electron ejection mechanisms characteristic to a specific range of impact velocities or projectile charges, the field is far from being well understood. Manifestations of dynamic or static electron-electron correlations have been examined even at the level of total ionization cross sections [12,14]. More details can be explored by measuring the angular and energy distribution of the emitted electrons which has become available recently due to an adaptation of the coincidence electron detection technique in the field. The so-called correlation functions [15,16], the role of first-order and second-order processes in the ejection mechanism [17] and some characteristic structures in the electron distributions [13]

have been the focus of the studies, while the threshold behavior of the DI process received less interest.

A positively charged heavy projectile can capture electron(s) of the He atom into its continuum (electron capture to the continuum, ECC) or, if it has electron(s) initially, they can also be transferred to the continuum due to the interaction with the target (electron loss to the continuum, ELC) (see [18] for more details). Both the ELC and the ECC mechanisms are manifested in a characteristic *cusp*-shaped peak in the energy and angular distribution of the ejected electron at a position where the velocity vector of the electron matches that of the projectile. The study of the cusp provides an extra opportunity to investigate the threshold effects, as the cusp electrons move with very low velocities relative to the projectile. The two-electron cusp peak was observed in a recent experiment for the 100 keV He^0 + He collision [19]. In the experiment the forward emission of two electrons from the process

$$He^0 + He \rightarrow He^+ + He^+ + e_1 + e_2, \tag{1}$$

(simultaneous ECC and ELC) was investigated. The process was identified by detecting coincidences between the two electrons and the outgoing, charge-state analyzed projectile.

For a 100 keV He projectile the velocity of the projectile $v_p = 1$ a.u., that is, the cusp appears at the electron energy $E_{\text{cusp}} = 1$ Ry. In the experiment, strong correlation was found between the energies of the ejected electrons: The emission of one electron with an energy smaller than E_{cusp} is accompanied preferentially by the emission of the other electron with energy larger than E_{cusp}. The observed energy correlation corresponds to an angular correlation of 180° in the projectile-centered reference frame. The preferred back-to-back emission of the electrons indicates the formation of Wannier-type correlated two-electron final states around the projectile in the collision.

In this work we investigate theoretically the two-electron ejection into the projectile's continuum in He^{2+} + He collisions. Since the projectile brings no electron into the collision, the cusp peak is formed due to the ECC mechanism only. Previous studies on the correlation function have shown that it is the final-state *e-e* interaction that primarily determines the energy and angular distribution of the DI electrons [15,16]. The final state of the process (1) investigated in the experiment and that of the double ECC studied in this work are similar: Two repelling electrons move in the attractive Coulomb field of a heavy charged particle in the same direction with small relative velocity. Therefore, we might expect that the present theoretical work reveals the main features of the two-electron cusp observed in the experiment.

The paper is organized as follows. Section II gives a brief overview of the basis of the theoretical models applied in the description of the process. Details of the models and a discussion of the results are presented in Sec. III. Conclusions are drawn in Sec. IV. Atomic units are used throughout the paper, except when otherwise stated.

II. THEORY

Let us consider DI of a helium atom by impact of a He^{2+} ion

$$He^{2+} + He(1s^2) \rightarrow He^{2+} + He^{2+} + e_1(\mathbf{k}_1) + e_2(\mathbf{k}_2), \tag{2}$$

where $\mathbf{k}_i$ denotes the momentum of the ith emitted electron with respect to the target nucleus (note the terms e_1 and e_2 are used only as convenient labels as the outgoing electrons are indistinguishable). Since we would like to describe the two-electron emission in the cusp region, it is crucial to include the interaction between the projectile and the electrons in the final state [18]. In principle, we face a *four-body* breakup scattering problem in which the interaction between the particles is the long-range Coulomb force. The case of the single cusp-electron emission is efficiently treated by the *continuum distorted wave* (CDW) method that accounts for the ECC cusp by applying the correct boundary conditions for the underlying three-body scattering problem. Similarly, for the exact description of the two-electron cusp the knowledge of the appropriate four-body boundary condition is unavoidable. In the lack of such a four-body theory, in the present work we attempted to find a solution to the problem in a way that we express the two-electron ionization amplitudes with one-electron amplitudes determined by a variant of the CDW method, and for the inclusion of the electron correlation we use some simplified forms of the 3C and DS3C approximations.

The basic assumptions of our model are as follows. Due to the high incident energy of the projectile for the present interest (100 keV in the experiment of Sarkadi and Orbán [19]) and the small energy transferred to the atom, the projectile can be considered as moving on a straight-line trajectory characterized by constant velocity $\mathbf{v}_p$ and impact parameter $\mathbf{b}$ (*impact parameter* approximation, IPA). Furthermore, since in this study we focus on the emission of electrons with small relative momentum ($k_{12} = |\mathbf{k}_1 - \mathbf{k}_2| < 1$), their interaction (correlation) time $t_{\text{corr.}}$ is much larger than the collision time $t_{\text{coll.}}$. The fulfillment of the condition $t_{\text{coll.}}/t_{\text{corr.}} \ll 1$ means that we may apply the *frozen-correlation* approximation (FCA, Martín and Salin [20]). In the FCA the electronic correlation in the asymptotic initial and final states is separated from those that may be present during the collision.

We describe the initial ground state of the He atom by a configuration interaction (CI) wave function as given by Silverman *et al.* [21]

$$\Phi_0(\mathbf{x}_1,\mathbf{x}_2) = \sum_{j_1 j_2} C_{j_1 j_2} \phi^{j_1}(\mathbf{x}_1)\phi^{j_2}(\mathbf{x}_2). \tag{3}$$

$\Phi_0(\mathbf{x}_1,\mathbf{x}_2)$ includes both the radial and angular correlations and yields 80% of the total correlation energy. $\mathbf{x}_i$ denotes the position of the ith electron. $\phi^{j_i}(\mathbf{x}_i)$'s are normalized hydrogen-like orbitals with optimized effective charges. The $C_{j_1 j_2}$ parameters are available for both single (only radially) and angularly correlated configurations for the initial state [21].

For the final two-electron continuum state we start from the following (approximate) ansatz:

$$\Phi_{\mathbf{k}_1\mathbf{k}_2}(\mathbf{x}_1,\mathbf{x}_2) = \frac{1}{\sqrt{2}}\big[(\phi_{\mathbf{k}_1}(\mathbf{x}_1)\phi_{\mathbf{k}_2}(\mathbf{x}_2) + \phi_{\mathbf{k}_1}(\mathbf{x}_2)\phi_{\mathbf{k}_2}(\mathbf{x}_1)\big]\varphi_{\mathbf{k}_1\mathbf{k}_2}(\mathbf{x}_1,\mathbf{x}_2). \tag{4}$$

Here the continuum orbitals $\phi_{\mathbf{k}_i}(\mathbf{x})$'s are also hydrogen-like wave functions but with a single effective charge $Z_{\text{eff}} = 1.67$. In our previous work [16] we found that the latter choice of Z_{eff} provides a more realistic description of the free electrons

in the field of the He^{2+} nucleus than the use of the optimized charges of the ground-state CI wave functions.

In our model the final-state correlation is incorporated via the function $\varphi_{\mathbf{k}_1\mathbf{k}_2}(\mathbf{x}_1,\mathbf{x}_2)$ appearing in Eq. (4). We might use the correlation function of the 3C model which depends on the relative position and momentum vectors of the two electrons [7]

$$\varphi_{\mathbf{k}_1\mathbf{k}_2}(\mathbf{x}_1,\mathbf{x}_2) = e^{-\pi Z_{12}/(2k_{12})}\Gamma(1 - iZ_{12}/k_{12})_1F_1(iZ_{12}/k_{12};1; -i(k_{12}x_{12} + \mathbf{k}_{12}\cdot\mathbf{x}_{12})), \quad (5)$$

where $\mathbf{x}_{12} = \mathbf{x}_1 - \mathbf{x}_2$ and $\mathbf{k}_{12} = \mathbf{k}_1 - \mathbf{k}_2$. However, the evaluation of the scattering amplitude in this case would represent a formidable task because of the dependence of the final-state wave function on $\mathbf{x}_{12}$. As a further, enormous simplification of our model we therefore assume that the electron-electron correlation can be expressed merely by a function of the *momentum vectors* of the electrons [i.e., $\varphi_{\mathbf{k}_1\mathbf{k}_2}(\mathbf{x}_1,\mathbf{x}_2) \approx \varphi(\mathbf{k}_1,\mathbf{k}_2)$]. With this approximation the cross-section differential with respect to the momenta of the ejected electrons can be written as

$$\frac{d\sigma}{d\mathbf{k}_1 d\mathbf{k}_2} = \frac{d\sigma^{\mathrm{IPM}}}{d\mathbf{k}_1 d\mathbf{k}_2}|\varphi(\mathbf{k}_1,\mathbf{k}_2)|^2. \quad (6)$$

Here $d\sigma^{\mathrm{IPM}}/d\mathbf{k}_1 d\mathbf{k}_2$ is a cross section calculated in the *independent particle model* (IPM). In the impact parameter approximation we may write

$$\frac{d\sigma^{\mathrm{IPM}}}{d\mathbf{k}_1 d\mathbf{k}_2} = \int d\mathbf{b}\left|a^{2e}_{i\to\mathbf{k}_1,\mathbf{k}_2}(\mathbf{b})\right|^2, \quad (7)$$

where the DI amplitude $a^{2e}_{i\to\mathbf{k}_1,\mathbf{k}_2}(\mathbf{b})$ can be expressed in the IPM as [16,20]

$$a^{2e}_{i\to\mathbf{k}_1,\mathbf{k}_2}(\mathbf{b}) = \frac{1}{\sqrt{2}}\sum_{j_1 j_2} C_{j_1 j_2}\left[a^{1e}_{j_1\to\mathbf{k}_1}(\mathbf{b})a^{1e}_{j_2\to\mathbf{k}_2}(\mathbf{b}) + a^{1e}_{j_1\to\mathbf{k}_2}(\mathbf{b})a^{1e}_{j_2\to\mathbf{k}_1}(\mathbf{b})\right]. \quad (8)$$

Here $a^{1e}_{j_i\to\mathbf{k}_i}$'s are single-ionization amplitudes. For the determination of the latter quantities we used a variant of the CDW model, the *continuum distorted-wave with eikonal initial-state* (CDW-EIS) approximation [22,23].

We note that the notation "IPM" in the cross section $d\sigma^{\mathrm{IPM}}/d\mathbf{k}_1 d\mathbf{k}_2$ is not completely correct because $d\sigma^{\mathrm{IPM}}/d\mathbf{k}_1 d\mathbf{k}_2$ still includes the initial-state correlation. However, comparison of the cross section (7) evaluated with $\Phi_0(\mathbf{x}_1,\mathbf{x}_2)$ belonging to a radially correlated, *single* CI configuration with that calculated with $\Phi_0(\mathbf{x}_1,\mathbf{x}_2)$ belonging to the angularly correlated CI configurations showed that the angular correlation in the initial state plays a negligible role in DI. The change of the cross section obtained with the single configuration CI wave function was less than 0.1% when the angular correlation was also included. Furthermore, test calculations show that the analysis of the problem of the two-electron cusp with uncorrelated OPM (optimized potential model) initial orbitals (see [16]) would result in the same conclusions.

In our analysis of DI in the cusp region we used various approximations for the correlation function $\varphi(\mathbf{k}_1,\mathbf{k}_2)$ in Eq. (6), the specific forms of which will be shown in the next section together with the presentation of the obtained results. To avoid any confusion, we note that we use the name "correlation function" for the correlation part of the final-state wave function (4) (i.e., the meaning of the correlation function in this work differs from that introduced by Schulz *et al.* [15] for the general characterization of the correlated emission of two electrons).

III. RESULTS

The cross-section differential in momenta of the ejected electrons can be transformed to the form differential in the energy and ejection angle of the electrons by the relationship

$$\frac{d\sigma}{dE_1 d\Omega_1 dE_2 d\Omega_2} = k_1 k_2 \frac{d\sigma}{d\mathbf{k}_1 d\mathbf{k}_2}, \quad (9)$$

where $d\Omega_i = \sin\theta_i\, d\theta_i\, d\varphi_i$. We evaluated the six-fold differential cross section (9) for DI of helium by He^{2+} projectiles at 100 keV impact energy. The single-ionization amplitudes $a^{1e}_{j_i\to\mathbf{k}_i}$ in (8) have been calculated for electron energies E_i $(=1/2k_i^2)$ from 0 to 50 eV in a wide range of the impact parameter $(0 \leqslant b \leqslant 20)$ and in the whole range of the ejection angles $(0 \leqslant \theta_i \leqslant 180^\circ)$.

Figure 1 shows the results of our calculations in the cusp region (8 eV $\leqslant E_i \leqslant$ 20 eV and $\theta_i = 0^\circ$) carried out with different correlation functions $\varphi(\mathbf{k}_1,\mathbf{k}_2)$ in Eq. (6), as well as the experimental data in the form of contour plots. Since we are mainly interested in the correlation property of the two-electron emission, we plot only relative cross sections.

In Fig. 1(a) the results obtained with $|\varphi(\mathbf{k}_1,\mathbf{k}_2)|^2 = 1$ (i.e., the predictions of IPM) are seen. The uncorrelated emission of the electron pairs is characterized by two ridges. The ridges are perpendicular straight lines ($E_1 = 13.6$ eV and $E_2 = 13.6$ eV). The cusp appears at the crossing point of the ridges.

As a first attempt, we tried to include the electron correlation by the so-called *Coulomb density of states* (CDS) approximation. CDS is a simplified version of the 3C model, assuming that a good account of the correlation can be obtained by the Coulomb normalization factor in Eq. (5)

$$|\varphi(\mathbf{k}_1,\mathbf{k}_2)|^2 = \frac{Z_{12}}{k_{12}}\frac{2\pi}{e^{2\pi Z_{12}/k_{12}} - 1}. \quad (10)$$

CDS has been successfully applied in numerous investigations [16,24–26] for the description of DI. A striking feature of this approximation is that it tremendously reduces the probability of the emission of two electrons into the same direction and with the same velocities $[|\varphi(\mathbf{k}_1,\mathbf{k}_2)|^2 \to 0$, as $k_{12} \to 0]$. Consequently, by including the electron correlation by the CDS, one expects a strong decrease of the two-electron cusp. Although we were aware of this property of CDS, we hoped that due to the diverging cross section for the cusp at the matching velocity, the peak would not disappear completely. However, as it is seen in Fig. 1(b), this was not the case: The cross section has a deep minimum along the line $E_1 = E_2$.

As noted in the Introduction, the 3C model fails to describe the electron emission above the threshold region. This is related to the fact that the interaction strength between the two continuum electrons, which is fixed by setting $Z_{12} = 1$, yields too strong a repulsion between the two low-energy electrons so that the cross sections are highly underestimated. This failure was corrected by introducing an effective charge that depends on the momenta of both electrons [10]. Different explicit forms of such DS3C models have been proposed (see, e.g., [27] and references therein) and applied mainly to the

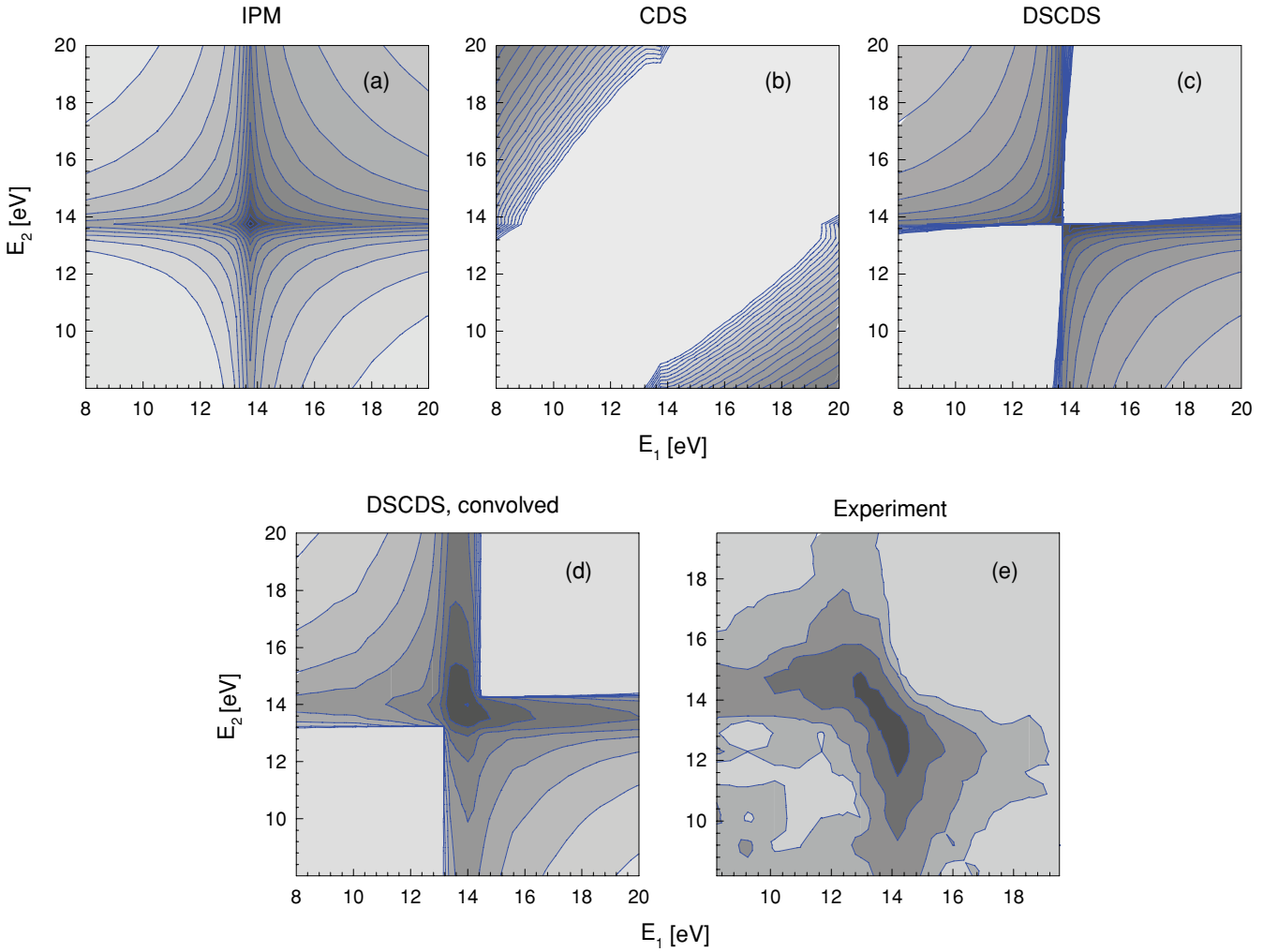

FIG. 1. (Color online) Panels (a–d): Contour plots of calculated relative six-fold differential cross sections for DI of He under 100 keV He^{2+} impact as functions of the electron ejection energies E_1 and E_2 at fixed ejection angles: $\theta_1 = \theta_2 = 0^\circ$ and $\varphi_1 = \varphi_2 = 0^\circ$. Theories: (a) Independent particle model (IPM); (b) Coulomb density of states model (CDS); (c) Dynamically screened CDS with a correlation function centered on the projectile (DSCDS); (d) Convoluted DSCDS (see text). Panel (e): Experimental data of Sarkadi and Orbán [19] for the process given by Eq. (1). The scale of the plots is logarithmic, the cross section between the neighboring contour levels changes by a factor of 2. The intensity increases with increasing tone of darkness.

description of electron-induced single ionization processes. As in our previous study [16], in the present work we also rely on a somewhat simplified derivation of the DS3C model by using

$$Z_{12} = 1 - \frac{k_{12}^2}{(k_1 + k_2)^2}, \tag{11}$$

which has been proposed and applied to $(e,3e)$ reactions [11]. Our calculations based on Eqs. (10) and (11), however, did not result in an improvement in the description of the two-electron cusp. We obtained again a deep minimum along the line $E_1 = E_2$.

Before going further it is worth referring to the theoretical description of the one-electron ECC process. This process cannot be accounted for in the first Born approximation where the ionization is viewed as an excitation from a bound state to a continuum state of the target [28]. To explain the ECC phenomenon in the B1 approximation the final continuum state must be centered on the projectile [29], that is, the interaction of the electron with the projectile plays the determining role in forming the final state. However, in this treatment the descriptions of the other ejection mechanisms (binary, etc. . .), fail or become less accurate. A consistent description of the single ionization and the ECC mechanism can be given within the framework of the CDW approximations [22,30]. In this treatment both the projectile and the target fields are treated on an equal footing and the chosen final wave function of the electron does not discriminate between the centers from which the ejection mechanism is viewed. Similarly, a consistent description of the two-electron ECC process would be given in a model where all the interactions of a given electron with the other aggregates were treated on an equal footing and where the discrimination between the centers of observation would not appear. As it will be seen, this is not fulfilled in the present treatment.

The application of the CDW-EIS theory in our model means that the two electrons move in the combined potential of

the target and projectile ions. However, with the $\varphi(\mathbf{k}_1,\mathbf{k}_2)$ approximations their correlated motion pertains to the field of the *target nucleus*. In the double cusp phenomenon, as in the single-electron case, the dominant interaction is between the outgoing *projectile* and the electron(s), while the target nucleus has only a perturbing effect. This means that in a more realistic theory of the two-electron cusp one would need a correlation function that describes, above all, the correlated motion of the two electrons in the field of the projectile. On the other hand, $\varphi(\mathbf{k}_1,\mathbf{k}_2)$ should also reflect the correlation due to the interaction of the electrons with the target from which they are ejected. Of course, the latter correlation plays a less important role in the process.

On the basis of the previous considerations we propose the following model. We neglect the correlation due to the interaction of the ejected electrons with the target. For the description of the correlated motion of the electrons in the field of the projectile we apply the simplified version of the DS3C model with a correlation function that depends on the momenta of the electrons measured *relative to the projectile*, $\mathbf{k}'_1,\mathbf{k}'_2$

$$\frac{d\sigma}{d\mathbf{k}_1 d\mathbf{k}_2} = \frac{d\sigma^{\mathrm{IPM}}(\mathbf{k}_1,\mathbf{k}_2)}{d\mathbf{k}_1 d\mathbf{k}_2} |\varphi(\mathbf{k}'_1,\mathbf{k}'_2)|^2, \tag{12}$$

with

$$|\varphi(\mathbf{k}'_1,\mathbf{k}_2)|^2 = \frac{Z_{12}}{k'_{12}} \frac{2\pi}{e^{2\pi Z_{12}/k'_{12}} - 1}, \tag{13}$$

and

$$Z_{12} = 1 - \frac{k'^2_{12}}{(k'_1 + k'_2)^2}. \tag{14}$$

Here $\mathbf{k}'_i = \mathbf{k}_i - \mathbf{v}_p$. In the following we refer to the above CDS model based on a projectile-centered dynamically screened correlation function by the abbreviation DSCDS. The predictions of DSCDS are shown in Fig. 1(c). The model is in accordance with the experimental finding in the respect that it predicts extremely small cross sections for the simultaneous emission of the electrons both having energies smaller or higher than E_{cusp}. This behavior can be understood considering that Eqs. (13) and (14) allow practically only back-to-back emission of the electrons in the projectile-centered reference frame.

From a theoretical point of view our procedure based on Eqs. (12) through (14) can be justified as follows. The CDW-EIS theory applied in $d\sigma^{\mathrm{IPM}}/d\mathbf{k}_1 d\mathbf{k}_2$ is capable of describing the *two-center* character of the electron emission (i.e., it can be considered as a more or less symmetric theory of ionization with respect to the target and projectile), that is, the cross sections are Galilean invariant. The three interacting particles for which the 3C wave function can be used for the inclusion of the *e*-*e* correlation in the final state are the target or the projectile nucleus and the two ejected electrons. However, as these different centers are not treated consistently in our model, the cross sections evaluated in the projectile and target frames are different [see Figs. 1(b) and 1(c) with the note that the DSCDS and CDS models are practically indistinguishable when the correlation function is centered on the target], that is, the Galilean or translational invariance of the treatment breaks. This means that the choice of the three particles of the 3C approach is arbitrary, it depends on the physical situation. For the description of the two-electron cusp it is natural to choose the projectile and the two electrons, as an ensemble of the dominantly interacting three particles in the final state.

Since in the vicinity of the cusp the cross section changes rapidly with the emission angle and the energy of the electrons, one cannot compare the theoretical results directly with the experimental data. To make a comparison between the theory and experiment, one has to integrate the theoretical cross section over the solid angles suspended by the detectors used in the experiment, as well as to convolute it with the spectrometer function to take into account the finite resolution of the energy measurement. The contour plot of the DSCDS cross section that includes the effect of the finite electron detection angles and energy resolution of the experiment by Sarkadi and Orbán [19] is seen in Fig. 1(d). The distribution clearly shows a peak at $E_1 \approx E_2 \approx E_{\mathrm{cusp}}$ (i.e., the cusp does not vanish when the electron-electron repulsion is switched on). The same theoretical results together with the experimental data are also displayed in a three-dimensional representation in Fig. 2. The scale of the latter plot is linear.

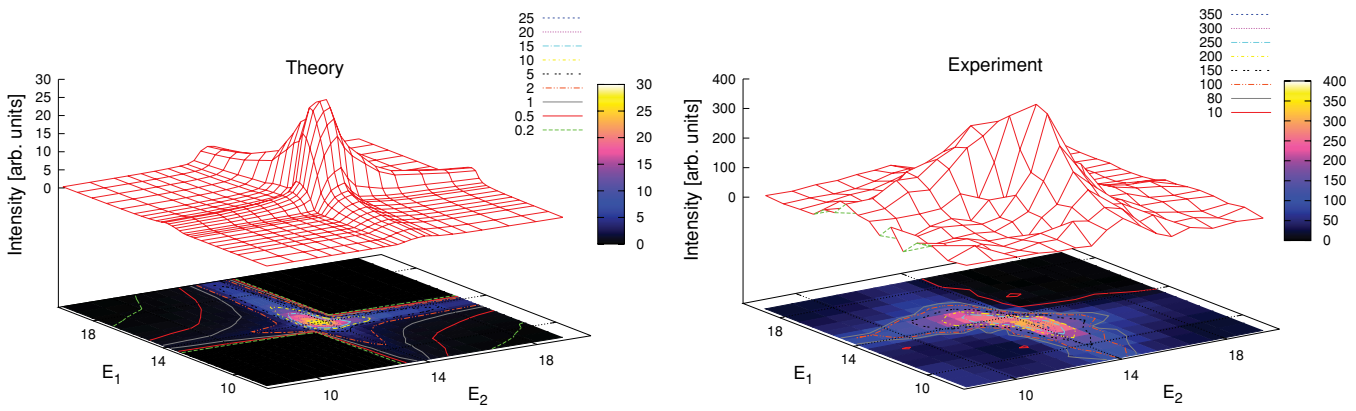

FIG. 2. (Color online) Two-electron emission distributions following DI of He under 100 keV He^{2+} impact as a function of the electron ejection energies E_1 and E_2 at $\theta_1 = \theta_2 = 0^\circ$. Left panel: Convoluted DSCDS (see text). Right panel: Experimental data of Sarkadi and Orbán [19] for the process given by Eq. (1).

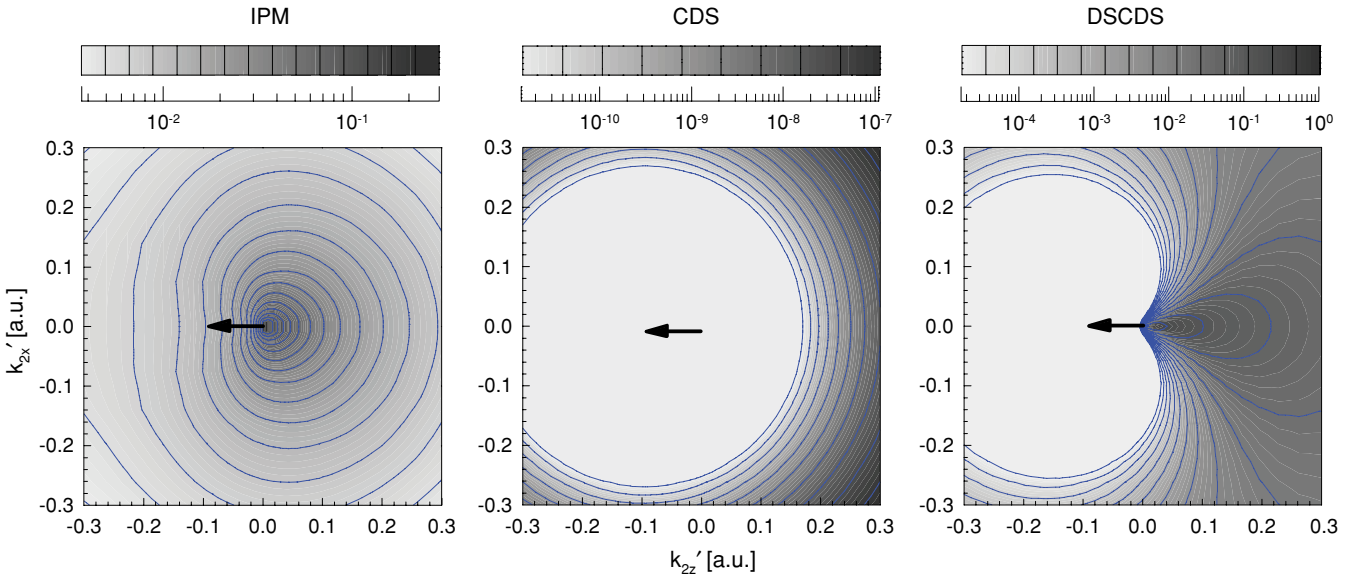

FIG. 3. (Color online) Contour plots of calculated six-fold differential cross sections for DI of He under 100 keV He^{2+} impact in the projectile-centered reference frame as functions of the momentum coordinates k'_{2x} and k'_{2z} of the electron e_2 at a fixed momentum vector of the electron e_1, $(k'_{1x},k'_{1z}) = (0, -0.086)$, and at relative azimuthal angle $\varphi_{k1}{}' - \varphi_{k2}{}' = 0^\circ$. Left, middle, and right panel: IPM, CDS, and DSCDS theory, respectively. The arrow shows the momentum vector of e_1.

Figure 3 illustrates the effect of adding the *e-e* correlation to the IPM by the CDS and DSCDS model. In the figure the contour plot of the sixfold differential cross section is shown in the *projectile*-centered reference frame with the following condition: The momentum of one of the electrons (e_1) is fixed at $(k'_{1x},k'_{1z}) = (0, -0.086)$, and the cross section is plotted as a function of the momentum of the other electron, e_2. Here the axis z' of the coordinate system is defined by the direction of the projectile beam. The data are plotted for relative azimuthal angle $\varphi_{k1}{}' - \varphi_{k2}{}' = 0^\circ$ (for other values of $\varphi_{k1}{}' - \varphi_{k2}{}'$ we obtained very similar cross-section values). In CDS the correlation function depends only on the relative electron momenta, $k_{12} = k'_{12}$, therefore it modifies the IPM cross sections isotropically. The strong *e-e* repulsion predicted by this model completely destroys the cusp seen in the contour plot of IPM. In DSCDS the correlation function depends also on k'_1 and k'_2, therefore the distribution becomes asymmetric. For example, for back-to-back emission $Z_{12} = 0$ [see Eq. (14)], that is, the charges of the electrons are completely screened. As a result of the reduced repulsion, the cusp does not vanish.

For a further investigation of the performance of the DSCDS model let us consider some selected ranges of the two-electron emission patterns shown in Figs. 1 and 2. In Fig. 4 we plotted the energy spectra of one of the ejected electrons, say e_1, with the condition that the energy of the other electron, e_2, lies in a narrow range (we may call it "coincidence window"). Panels (a), (b), and (c) belong to three different coincidence windows. The spectra are normalized at their maxima. In the figure we compare spectra calculated with and without the inclusion of the electron correlation in the frameworks of DSCDS and IPM, respectively. Of course, in IPM the shape of the cusp is identical for all three coincidence windows. At the same time, the shape and the position of the cusp obtained in DSCDS depend sensitively on E_2. In panel (a) the coincidence window is set at the low-energy wing of the cusp. As a result of the correlation, the peak in this case is shifted to higher energies and the shape of the cusp becomes more asymmetric due to the strong decrease of the emission probability for $E_1 < E_{\text{cusp}}$. In panel (c), where the coincidence window is set at the high-energy wing of the cusp, an opposite behavior can be observed when the correlation is switched on. In panel (b) E_2 is fixed at the peak maximum. The inclusion of the correlation in this case has only a small effect on the shape and the position of the cusp. In the figure we also plotted the experimental data of Sarkadi and Orbán [19]. DSCDS reflects reasonably well the tendencies of the energy correlation found in the experiment: The direction of the shifts of the peak and that of the changes of the peak asymmetry are well reproduced by the theory. However, the agreement with the experiment is only qualitative. The theory largely underestimates the asymmetry of the cups in cases (b) and (c). Furthermore, while the intensities of the peaks measured in the experiment are almost the same, the cusp predicted by DSCDS in case (a) is smaller by one order of magnitude than that in cases (b) and (c).

The discrepancies between theory and experiment can be related to the following: (i) The mechanism of the formation of the two-electron cusp in the both cases is different, it is double ECC for He^{2+} projectiles considered in the present work, and simultaneous ECC and ELC for He^0 projectiles in the experiment. (ii) The asymmetry of the ECC peak is described by the CDW-EIS theory incorrectly, even for single ionization. (iii) The treatment of the *e-e* correlation in the present theoretical model is rather crude.

The failure of CDW-EIS in describing the shape of the cusp for single ionization is demonstrated in Fig. 5, where the ECC cusp predicted by this theory is compared with that measured in one of our previous experiments for 100 keV He^{2+} + He collision [31]. In the experiment the electrons

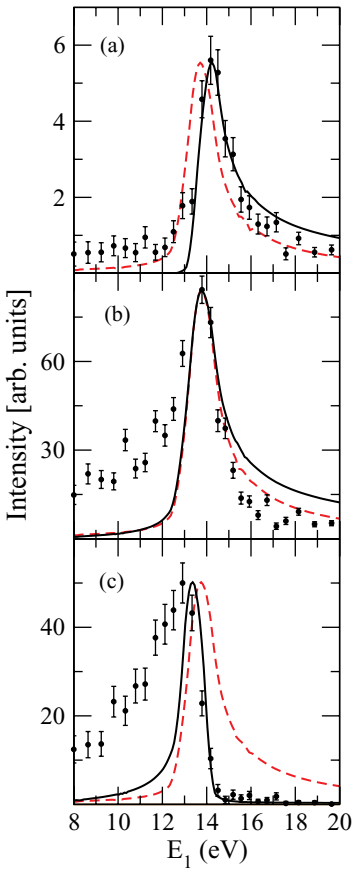

FIG. 4. (Color online) Energy spectra of the electron e_1 in the laboratory frame at $\theta_1 = \theta_2 = 0^\circ$ for 100 keV He^{2+} + He collision. The curves are the results of the present calculations obtained by convoluting the theoretical cross sections with the energy and angular resolution of the experiment by Sarkadi and Orbán [19]. Solid line: DSCDS; dashed line: IPM. Closed circles: Experimental data for the process shown in Eq. (1). For the spectra in panels (a), (b), and (c) the energy of e_2 lies in the intervals 11.0–12.5 eV, 13.0–14.2 eV, and 14.5–16.0 eV.

were detected in coincidence with the outgoing He^{2+} ions to exclude the contribution from the transfer ionization channel. As is seen, the measured peak is strongly skewed to lower energies, while the theoretical one is almost symmetric. The skewness of the peak toward lower energies is a well known property of the ECC cusp [18,32]. Theoretically it is explained as a higher-order effect [33], or as a result of the simultaneous interaction of the emitted electron with the projectile and the residual ion [34]. The bad performance of CDW-EIS concerning the shape of the ECC cusp is not fully understood. The CDW theory in its original form predicts the correct peak shape, however, it highly overestimates the cross section at low impact velocities due to improper normalization [22,35]. In CDW-EIS the introduction of the eikonal approximation for the distortion of the entrance channel resolves the normalization failure of CDW, however, it gives rise to an incorrect cusp shape. The almost symmetric peak predicted by CDW-EIS means that the electron emission with respect to the projectile is almost isotropic, that is, the population of the continuum states characterized by high angular momenta around the projectile is strongly underestimated by the theory [33,36].

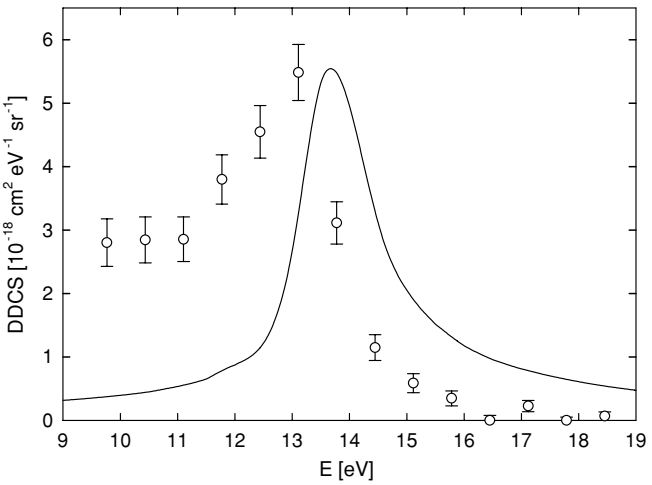

FIG. 5. The ECC cusp for single ionization of He by impact of 100 keV He^{2+} ions. The curve and the points are results of CDW-EIS calculations and experimental data [31], respectively. The experimental data are normalized at the maximum of the theoretical curve.

One can hardly understand why the latter effect is caused by the eikonal approximation applied for the distortion of the entrance channel. Both CDW and CDW-EIS describe the electron emission in the two-center potential formed by the projectile and the target core [37], therefore the correct cusp shape is expected for both theories.

From the previous considerations it follows that the use of CDW for the treatment of the double ionization (instead of CDW-EIS) would probably substantially reduce the discrepancies between the shapes of the measured and calculated two-electron cusp. With the use of CDW the IPM curves seen in Fig. 4 are expected to be skewed to lower electron energies, and consequently the DSCDS curves would also be enhanced at the low-energy wing of the cusp. In the present work we used CDW-EIS in the lack of a CDW theory that is suitable for the treatment of the double ionization. Furthermore, our aim was only to confirm the existence of the two-electron cusp, and to give a theoretical support to the observed correlation between the energies of the two electrons.

An interesting feature of the two-electron emission can be seen in the right panel of Fig. 3. Close to the cusp maximum the cross section varies very rapidly with the emission angle of the electron e_2. The strong angular dependence of the electron emission in the projectile frame is manifested in a drastic change of the energy spectrum in the laboratory frame as a function of the observation angle around 0°. This is shown in Fig. 6 where energy spectra of e_1 at laboratory observations angles 0°, 0.125°, 0.25°, and 0.5° are plotted with the condition that e_2 is ejected with energy $E_2 = 12$ eV and at angle $\theta_2 = 0^\circ$. As is seen, the peak is shifted and broadens with increasing observation angle. The energy shifts and the changes of the asymmetry of the cusp observed both experimentally and in the present theoretical calculations for a *finite* acceptance angle (see Fig. 4) can be traced back to the behavior of DI seen in Fig. 6. The analysis of our DSCDS data shows that doubling the size of the angular acceptance results in a three times larger shift of the peak.

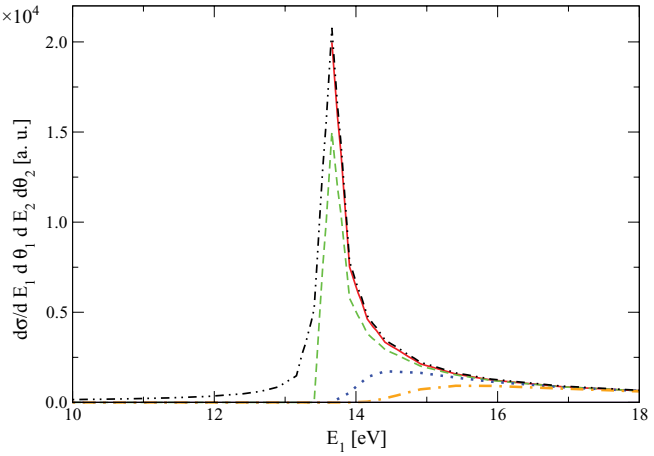

FIG. 6. (Color online) Four-fold differential cross sections in the laboratory frame as a function of ejection energy E_1 for 100 keV He^{2+} + He collisions at $E_2 = 12$ eV and at $\theta_2 = 0°$. The curves are results obtained in the framework of DSCDS and IPM. DSCDS: $\theta_1 = 0°$, solid line; $\theta_1 = 0.125°$, dashed line; $\theta_1 = 0.25°$, dotted line; $\theta_1 = 0.5°$, dot-dashed line. IPM: $\theta_1 = 0°$, dot-dot-dashed line.

IV. CONCLUSION

We investigated the existence of the two-electron cusp theoretically. We considered the simplest collision system in which the phenomenon can be observed (i.e., the collision of He^{2+} ions with He atoms). In this system the two-electron cusp may be formed via double ECC. Applying the frozen-correlation approximation, we treated the one-electron ionization events by the CDW-EIS theory, and for the description of the electron correlation in the final state we used simplified forms of the 3C and DS3C approximations. The main physical issue of the present work is the outcome of the competition between two interactions (i) The repulsion between the two ejected electrons, and (ii) the strong final-state (Coulomb-focussing) interaction between the electrons and the outgoing projectile. Our calculations carried out at 100 keV impact energy have shown that in the 3C approximation the two-electron cusp does not exist. Considering that the cusp is a threshold phenomenon in the projectile-centered reference frame, our finding is in accordance with earlier observations, namely that the 3C model is unable to account for the two-electron emission in the threshold region where the Wannier mechanism plays an important role [2].

By applying a projectile-centered DS3C correlation function, our calculations showed the existence of a two-electron cusp. The shift and the asymmetry of the cusp under special coincidence conditions were found to be in qualitative agreement with those observed by Sarkadi and Orbán [19] in He^0 + He collisions. The similarity of the results obtained for the He^{2+} projectile of the present work and for the He^0 projectile of the experiment emphasizes the importance of the *e-e* interaction in the final state: The spectral distribution of the two-electron emission in the cusp region is dominantly determined by the angular correlation of 180° between the electrons in the final state.

The double ECC process is a real four-body problem (which is hard to reduce to a three-body or two-body problem): Besides the dominant interaction of the two outgoing ionized electrons with each other and with the projectile one cannot neglect the interaction of the electrons with the double-ionized target in the final state [38]. A better understanding of the phenomenon of the two-electron cusp could be achieved by an extension of the CDW method that applies a correct four-body boundary condition. In our treatment we applied a dynamically screened effective charge only for the *e-e* interaction, where its role proved to be essential. The effects of such effective charges in case of the electron projectile/target interactions are not obvious, and require more computational efforts that we plan to implement as an extension of this work. Further experimental data are also needed, first of all for the collision system studied in the present work.

ACKNOWLEDGMENTS

This work was supported by the National Scientific Research Foundation and the National Office for Research and Technology of Hungary (NKTH-OTKA, Grants No. K67719 and K73703).

[1] J. Berakdar, A. Lahmam-Bennani, and C. D. Cappello, Phys. Rep. **374**, 91 (2003).
[2] J. S. Briggs and V. Schmidt, J. Phys. B **33**, R1 (2000).
[3] S. Keller, B. Bapat, R. Moshammer, J. Ullrich, and R. M. Dreizler, J. Phys. B **33**, 1447 (2000).
[4] A. Kheifets, I. Bray, A. Lahmam-Bennani, A. Duguet, and I. Taouil, J. Phys. B **32**, 5047 (1999).
[5] L. U. Ancarani, T. Montagnese, and C. D. Cappello, *Electron and Photon Impact Ionisation and Related Topics*, edited by B. Piraux, IOP Conf. Proc. No. 183 (Institute of Physics, London, 2005), p. 21.
[6] C. R. Garibotti and J. E. Miraglia, Phys. Rev. A **21**, 572 (1980).
[7] M. Brauner, J. S. Briggs, and H. Klar, J. Phys. B **22**, 2265 (1989).
[8] G. H. Wannier, Phys. Rev. **90**, 817 (1953).
[9] J. M. Feagin, J. Phys. B **29**, L551 (1996).
[10] J. Berakdar and J. S. Briggs, Phys. Rev. Lett. **72**, 3799 (1994).
[11] J. R. Götz, M. Walter, and J. S. Briggs, J. Phys. B **38**, 1569 (2005).
[12] J. H. McGuire, *Electron Correlation Dynamics in Atomic Collisions*, Cambridge Monographs on Atomic, Molecular and Chemical Physics (No. 8), (Cambridge University Press, Cambridge, England, 1997).
[13] D. Fischer *et al.*, Phys. Rev. Lett. **90**, 243201 (2003).
[14] L. Gulyás, A. Igarashi, P. D. Fainstein, and T. Kirchner, J. Phys. B **41**, 025202 (2008).
[15] M. Schulz, R. Moshammer, W. Schmitt, H. Kollmus, B. Feuerstein, R. Mann, S. Hagmann, and J. Ullrich, Phys. Rev. Lett. **84**, 863 (2000).
[16] L. Gulyás, A. Igarashi, and T. Kirchner, Phys. Rev. A **74**, 032713 (2006).
[17] M. Schulz, M. F. Ciappina, T. Kirchner, D. Fischer, R. Moshammer, and J. Ullrich, Phys. Rev. A **79**, 042708 (2009).

[18] N. Stolterfoht, R. D. DuBois, and R. D. Rivarola, *Electron Emission in Heavy Ion-Atom Collisions* (Springer, Berlin, 1997).
[19] L. Sarkadi and A. Orbán, Phys. Rev. Lett. **100**, 133201 (2008).
[20] F. Martín and A. Salin, Phys. Rev. A **54**, 3990 (1996).
[21] J. N. Silverman, O. Platas, and F. A. Matsen, J. Chem. Phys. **32**, 1402 (1960).
[22] D. S. F. Crothers and J. F. McCann, J. Phys. B **16**, 3229 (1983).
[23] P. D. Fainstein, L. Gulyás, and A. Salin, J. Phys. B **29**, 1225 (1996).
[24] C. D. Cappello, B. Joulakian, and J. Langlois, J. Phys. (France) **3**, C6-125 (1993).
[25] J. Bradley, R. J. S. Lee, M. McCartney, and D. S. F. Crothers, J. Phys. B **37**, 3723 (2004).
[26] M. Fiori, A. B. Rocha, C. E. Bielschowsky, G. Jalbert, and C. R. Garibotti, J. Phys. B **39**, 1751 (2006).
[27] S. Zhang, J. Phys. B **33**, 3545 (2000).
[28] P. D. Fainstein, V. H. Ponce, and R. D. Rivarola, J. Phys. B **24**, 3091 (1991).
[29] J. E. Miraglia and V. H. Ponce, J. Phys. B **13**, 1195 (1980).
[30] D. Belkić, J. Phys. B **11**, 3529 (1978).
[31] L. Sarkadi, L. Lugosi, K. Tőkési, L. Gulyás, and Á. Kövér, J. Phys. B **34**, 4901 (2001).
[32] J. Burgdörfer, in *Lecture Notes in Physics*, edited by K. O. Groeneweld, W. Meckbach, and I. A. Sellin (Springer, Berlin, 1984), Vol. 213, p. 32.
[33] R. Shakeshaft and L. Spruch, Phys. Rev. Lett. **41**, 1037 (1978).
[34] J. Berakdar, Phys. Rev. Lett. **81**, 1393 (1998).
[35] P. Závodszky, L. Gulyás, L. Sarkadi, T. Vajnai, G. Szabó, S. Ricz, and J. Pálinkás, Nucl. Instrum. Methods Phys. Res. B **86**, 175 (1994).
[36] J. Burgdörfer, Phys. Rev. A **33**, 1578 (1986).
[37] D. S. F. Crothers and L. J. Dubé, in *Advances in Atomic, Molecular and Optical Physics* (Academic Press, New York, 1993), Vol. 30, p. 287.
[38] L. Sarkadi and A. Orbán, Nucl. Instrum. Methods B **267**, 270 (2009).